

STRONG: Synchronous and asynchronous RObust Network localization, under Non-Gaussian noise

Cláudia Soares*, João Gomes

*Institute for Systems and Robotics, Laboratory for Robotics and Engineering Systems, IST
Universidade de Lisboa, Portugal*

Abstract

Real-world network applications must cope with failing nodes, malicious attacks, or nodes facing corrupted data — data classified as outliers. Our work addresses these concerns in the scope of the sensor network localization problem where, despite the abundance of technical literature, prior research seldom considered outlier data. We propose robust, fast, and distributed network localization algorithms, resilient to high-power noise, but also precise under regular Gaussian noise. We use a Huber M-estimator, thus obtaining a robust (but nonconvex) optimization problem. We convexify and change the problem representation, to allow for distributed robust localization algorithms: a synchronous distributed method that has optimal convergence rate and an asynchronous one with proven convergence guarantees. A major highlight of our contribution lies on the fact that we pay no price for provable distributed computation neither in accuracy, nor in communication cost or convergence speed. Simulations showcase the superior performance of our algorithms, both in the presence of outliers and under regular Gaussian noise: our method exceeds the accuracy of alternative approaches, distributed and centralized, even under heavy additive and multiplicative outlier noise.

Keywords: Distributed Localization algorithms, Robust estimation, Huber function, convex relaxation, nonconvex optimization, distributed iterative network localization, sensor networks

1. Introduction

Outliers can cause large errors in non-robust estimation algorithms and, if other systems use wrong estimates as input, error propagation can invalidate the engineered system's final purpose. Network localization is a key component in many network-centric systems that is prone to such drastic error propagation.

*Corresponding author

Email addresses: csoares@isr.tecnico.ulisboa.pt (Cláudia Soares),
jgg@isr.tecnico.ulisboa.pt (João Gomes)

It might be taken for granted in most sensor network applications, but in challenging environments network localization is an open and very active research field. We present a new approach addressing the presence of outliers, not by eliminating them from the estimation process, but by weighting them, so they can contribute to the solution, while mitigating the outlier bias on the estimator. [This strategy is strongly rooted in Robust Statistics and Robust Statistical Signal Processing \[1\].](#)

1.1. Related work

Focusing on more related work, several different approaches are available, some performing semidefinite or second-order cone relaxations of the original nonconvex problem like Oğuz-Ekim *et al.* [2] or Biswas *et al.* [3]. These approaches do not scale well, since the centralized semidefinite program (SDP) or second-order cone program (SOCP) gets very large even for a small number of nodes. In Oğuz-Ekim *et al.* the Majorization-Minimization (MM) framework was used with quadratic cost functions to also derive centralized approaches to the sensor network localization problem. Other approaches rely on multidimensional scaling, where the sensor network localization problem is posed as a least squares problem, as in the excellent work of Shang *et al.* [4]. Unfortunately, multidimensional scaling is unreliable in large-scale networks with sparse connectivity. Another class of relaxations focuses on the envelopes of terms in the cost function, like the work in [5], where we present three algorithms for network localization, one parallel and two asynchronous ones, all with proven convergence. While developed as a relaxation of a maximum-likelihood estimator, [5] assumes an additive Gaussian noise measurement model which, as we now show through numerical simulations, does not withstand outlier noise. To address a data model where range measurements are contaminated with Gaussian measurement noise plus outliers, here we cast the localization problem in a broader M-estimation framework and replace the outlier-amplifying quadratic loss considered in [5] by the robust Huber function. A Huber M-estimator was already used for centralized target localization in [6], where the Huber estimation was used in a bootstrapping scheme. The robust problem is also nonconvex and a global optimum is very difficult to find. As in [5], we opt for a term-to-term relaxation, but unlike [5] the new convex approximated robust problem includes explicit constraints that elicit different solution methods. To find a distributed algorithm with low computational complexity, we put forward a novel representation of the Huber function composed with a norm. We start by developing an optimal first-order synchronous algorithm, similarly to [5], but for a different, robust problem. As network localization in many applications calls for unstructured, asynchronous time models, we also develop an asynchronous algorithm based on coordinate gradient descent, for which we provide proof of convergence to the optimal cost with probability one. This parallels the result in the unconstrained Gaussian-motivated problem in [5], but for the robust problem with constraints.

Some existing references directly tackle the nonconvex maximum-likelihood problem. Due to nonconvexity of the problem, such iterative algorithms can

be trapped in one of the multiple local maxima of the cost, and consequently they aspire to no more than finding a local optimum that may be highly sensitive to the algorithm initialization. Here we can point out several approaches, like Costa *et al.* [7], where the authors present a distributed solution inspired in multidimensional scaling, Ersenghe [8] that presents a nonconvex ADMM, proven to converge to a stationary point of the ML cost, and Soares *et al.* [9], where the authors reformulate the problem to obtain a Lipschitz gradient cost, decoupling the problem via MM. A common approach to initialize the nonconvex maximum-likelihood algorithms is to run a convex relaxation, and refine the result with the nonconvex method. This type of approach can be found in [10].

Some of the localization fundamental limits were object of thorough study, for example in [11], the authors derive closed-form Cramér-Rao bounds for multi-modal, multi-agent systems, with remarkably general assumptions, but only covering independent Gaussian noise. The very recent work [12] notes that the Cramér-Rao lower bound considered in previous research assumes a fixed configuration of anchoring nodes, thus not conveying the full picture regarding localization performance; to address this gap, the authors consider the bound as a random variable, and put forward the distribution of the Cramér-Rao lower bound under a time of arrival measurement model. The statistical assumptions on this result include, again, normally distributed independent measurement noise. The recent rise of 5G and full-duplex wireless communications opened the door to interesting developments in GPS-denied localization technologies, as in [13], and [14], both presenting fundamental bounds and estimators for position and orientation, once more assuming normally distributed noise.

All these approaches assume Gaussian noise contaminating the distance measurements or their squares, while many empirical studies reveal that real data are seldom Gaussian. Despite this, the literature is scarce in robust estimation techniques for network localization. Some of the few approaches rely on identifying outliers from regular data and discarding them. An example is Ihler *et al.* [15], which formulates network localization as an inference problem in a graphical model. To approximate an outlier process the authors add a high-variance Gaussian to the Gaussian mixtures and employ non-parametric belief propagation to approximate the solution. The authors assume a particular probability distribution for outlier measurements. In the same vein, Ash *et al.* [16] employs the EM algorithm to jointly estimate outliers and sensor positions, and Yin *et al.* [17] tackled robust localization in a wireless environment, assuming noise can only enter the process through propagation and not measurement hardware. Also, their method is designed for single source localization using a set of base stations, whereas we deal with the robust network localization problem. Their algorithms, EM- and JMAP-ML, performed estimation of the position, mixture parameters, and assumed an outlier noise model for unknown propagation conditions, again under predetermined probability distributions. Further, Yin *et al.* assume that several measurements are taken of the same distance. In our setup only one measurement is collected, for each underlying distance between elements..

Alternatively, methods may perform a soft rejection of outliers, still allowing

them to contribute to the solution. Oğuz-Ekim *et al.* [2] derived a maximum-likelihood estimator for Laplacian noise and relaxed it to a convex program by linearizing and dropping a rank constraint; they also proposed a centralized algorithm to solve the approximated problem. Such centralized solutions fail to scale with the number of nodes and number of collected measurements. Forero and Giannakis [18] presented a robust multidimensional scaling based on regularized least squares, where the regularization term was replaced by a convex function, and solved via MM. The main drawbacks of this approach are the centralized processing architecture and selection of a sensitive regularization parameter. Korkmaz and van der Veen [19] use the Huber loss [20] composed with a discrepancy function between measurements and estimated distances, in order to achieve robustness to outliers. The resulting cost is nonconvex, and optimized by means of the Majorization-Minimization technique. The method is distributed, but the quality of the solution depends on the quality of the initialization. The recent work of Chen and colleagues [21] puts forward a new model for LOS/NLOS based on a multiplicative transformation of the additive data model, considering Exponential noise. The authors argue that this type of noise is routinely found in dense urban areas. They also propose a relaxation of their proposed data model to be run distributedly via the ADMM framework—unlike our present work, where we are focusing on the standard noise model-agnostic Huber M-estimator. Yousefi *et al.* [22] present a distributed gradient algorithm for a Huber discrepancy relaxed problem. This is inspired by the Projection Onto Convex Sets approach of Blatt and Hero [23] for single source localization, later extended to network localization by Gholami *et al.* [24]. We independently developed the same relaxation (see also [25]), but whereas Yousefi *et al.* optimized it by means of a gradient method, our reformulation and analysis presented here leads to (i) a synchronous algorithm with optimal convergence, and (ii) a provably convergent asynchronous algorithm. These two modes are of paramount importance in real-world implementations, where fast methods clearly have an edge in the presence of time and power constraints, and the unstructured nature of engineered networks calls for asynchronous operation.

1.2. Contributions

In applications of large-scale networks there is a need for distributed localization methods with soft rejection of outliers that are simple to implement, scalable and efficient under reasonable outlier noise distributions. Our methods incorporate outliers into the estimation process and do not assume any statistical outlier model. We capitalize on the robust estimation properties of the Huber function but, unlike Korkmaz and van der Veen [19], we do not address the nonconvex cost in our proposal, thus removing the initialization uncertainty. Instead, we derive a convex relaxation which numerically outperforms relevant benchmark methods, and other natural formulations of the problem. The contributions of this work are:

1. We motivate a **tight convex underestimator** for each term of the robust discrepancy measure for sensor network localization (Section 3), and

we provide an **optimality bound** for the convex relaxation. Further, we analyze the tightness of the convex approximation. We also compare it with other discrepancy measures and appropriate relaxations. All measurements contribute to the estimate, although we do not compute specific weights. Numerical simulations illustrate the quality of the convex under-estimator (Section 3.1);

2. We develop a **distributed gradient method**, requiring only simple computations at each node, with **guaranteed optimal convergence rate** (Sections 4.4 and 5.1). The keystone of the algorithm is a new representation of the Huber function composed with a norm (Section 4.1).
3. Further, we introduce an **asynchronous method** for robust network localization, with convergence guarantees (Sections 4.5 and 5.2);

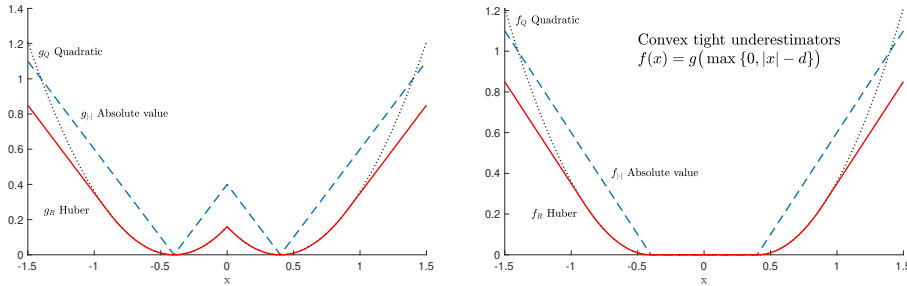
We benchmark our algorithms against published methods in robust network localization, achieving better performance with fewer communications (Section 6). The proposed scheme has optimal convergence rate for a first-order method, in the synchronous case, without degradation of accuracy. It does not require further approximation/relaxation for parallel operation, as it is naturally distributed. Both properties follow from our novel representation of the robust localization problem, as described in Sections 2 and 3. [The reduced communication cost for the distributed methods is due to having a cost whose gradient is naturally distributed and the only data needed to broadcast to neighbors is the current estimate of each node’s position. At each iteration a node only communicates a vector of the same size as the ambient space \(\$\mathbb{R}^2\$ or \$\mathbb{R}^3\$ \).](#)

2. Discrepancy measure

The network is represented as an undirected graph $\mathcal{G} = (\mathcal{V}, \mathcal{E})$, where $\mathcal{V} = \{1, 2, \dots, n\}$ indexes the set of sensors with unknown positions and \mathcal{E} is the set of edges. There is an edge $i \sim j \in \mathcal{E}$ between nodes i and j if a pairwise range measurement is available and i and j can communicate with each other. Anchors have known positions and are collected in the set $\mathcal{A} = \{1, \dots, m\}$; they are not nodes on the graph \mathcal{G} . For each sensor $i \in \mathcal{V}$, we let $\mathcal{A}_i \subset \mathcal{A}$ be the subset of anchors with measured range to node i . The set \mathcal{N}_i collects the neighbor sensor nodes of node i .

The element positions belong to \mathbb{R}^p , with $p = 2$ for planar networks and $p = 3$ for volumetric ones. We denote by $x_i \in \mathbb{R}^p$ the position of sensor i , and by d_{ij} the range measurement between sensors i and j . The variable $x = \{x_{\mathcal{V}}\}$ concatenates all unknown sensor positions. Anchor positions are denoted by $a_k \in \mathbb{R}^p$. We let r_{ik} denote the noisy range measurement between sensor i and anchor k . The given data are, thus, the anchor positions $\{a_k \in \mathbb{R}^p : k \in \mathcal{A}\}$, noisy ranges between sensors $\{d_{ij} : i \sim j \in \mathcal{E}\}$ and noisy ranges between sensors and anchors $\{r_{ik} : i \in \mathcal{V}, k \in \mathcal{A}_i\}$.

We wish to estimate the sensor positions taking into account two types of noise: (1) regular Gaussian noise, and (2) outlier-induced noise.



(a) For Gaussian noise, $g_Q(x)$, evidences steep tails acting as outlier amplifiers. The loss $g_{|\cdot|}(x)$, adapted to impulsive noise, fails to model the Gaussianity of low-power operating noise. The Huber loss $g_R(x)$ combines robustness to high-power outliers and adaptation to regular noise.

(b) All functions f are the convex envelopes and, thus, the best convex approximations of the functions g in Figure 1(a). The convexification is performed by restricting the arguments of g to be nonnegative.

Figure 1: The different cost functions considered in this paper, applied to a 1D problem with one node and one anchor. The anchor sits at the origin, and the node at 0.4, so $d = 0.4$ in the absence of noise. The scalar variable for the node position is denoted as x . The ML estimator for independent white Gaussian noise is $g_Q(x) = (|x| - d)^2$, while the ML estimator considering Laplacian noise is $g_{|\cdot|}(x) = ||x| - d|$. The Huber M-estimator is defined by $g_R(x) = h_{\delta=0.8}(|x| - d)$.

Outlier measurements are non-Gaussian and will heavily bias the solutions of the standard maximum-likelihood estimator for sensor positions with additive independent and identically distributed (i.i.d.) Gaussian noise, since their magnitude will be amplified by the squares in each outlier term. Robust estimation theory provides some alternatives to perform soft rejection of outliers, namely, replacing each quadratic loss above with the L_1 loss or the Huber loss, defined as

$$h_{\delta}(u) = \begin{cases} u^2 & \text{if } |u| \leq \delta, \\ 2\delta|u| - \delta^2 & \text{if } |u| \geq \delta. \end{cases} \quad (1)$$

The Huber loss achieves the best of two worlds: it is robust for large values of the argument — like the L_1 loss — and for reasonable noise levels it behaves like a quadratic, thus leading to the maximum-likelihood estimator adapted to regular noise [1]. Figure 1(a) depicts the different nonconvex costs g_Q , $g_{|\cdot|}$, g_R for Gaussian, L_1 and Huber losses, respectively, evaluated for a one-dimensional problem with one node and one anchor. We can observe in this simple example the main properties of the different cost functions, in terms of adaptation to low/medium-power Gaussian noise and high-power outlier spikes. Using (1) we can write our robust optimization problem as

$$\underset{x}{\text{minimize}} \quad g_R(x) \quad (2)$$

where

$$g_R(x) = \sum_{i \sim j} \frac{1}{2} h_{D_{ij}}(\|x_i - x_j\| - d_{ij}) + \sum_i \sum_{k \in \mathcal{A}_i} \frac{1}{2} h_{R_{ik}}(\|x_i - a_k\| - r_{ik}) \quad (3)$$

and D_{ij} , R_{ik} denote the chosen Huber radii for inter-node and node-anchor terms, which will be discussed in Section 6. This function is nonconvex and, in general, difficult to minimize. We shall provide a convex underestimator that tightly bounds each term of (3), thus leading to better estimation results than other relaxations such as [26]. The expected enhanced performance of our relaxation for the estimation under outlier noise comes naturally from the fact that our formulation directly accounts for it, whereas the one in [26] does not. The mismatch between the data model and data distribution can strongly impact the quadratic terms considered in the ML estimator for Gaussian noise. A thorough study of the impact of robust statistics in Signal Processing can be found in [1].

3. Convex underestimator

To convexify g_R we can replace each term by its convex hull¹, as depicted in Figure 1(b) following the same approach as in Falk and Soland [28] or, more recently, in our paper [5]. Here, we observe that the high-power behavior is maintained, whereas the medium/low-power is only altered in the convexified area. We define the convex costs by composing any of the convex losses with a non-decreasing function $(\xi)_+ = \max\{0, \xi\}$ which, in turn, operates on the discrepancies $\|x_i - x_j\| - d_{ij}$, and $\|x_i - a_k\| - r_{ik}$. As $(\|x_i - x_j\| - d_{ij})_+$ and $(\|x_i - a_k\| - r_{ik})_+$ are non-decreasing and each one of the functions $h_{D_{ij}}$ and $h_{R_{ik}}$ is convex, then their sum

$$f_R(x) = \sum_{i \sim j} \frac{1}{2} h_{D_{ij}} \left((\|x_i - x_j\| - d_{ij})_+ \right) + \sum_i \sum_{k \in \mathcal{A}_i} \frac{1}{2} h_{R_{ik}} \left((\|x_i - a_k\| - r_{ik})_+ \right) \quad (4)$$

is also convex, for any positive value of parameters D_{ij} for each edge $i \sim j$, and R_{ik} for each node-anchor pair $i \in \mathcal{V}, k \in \mathcal{A}_i$. The cost function (4) also appears in Yousefi *et al.* [22] via a distinct reasoning. The striking difference with respect to Yousefi *et al.* is how the cost (4) is exploited here to generate distributed solution methods where all nodes work in parallel with optimal first-order convergence speed, for the synchronous algorithm, or randomly awoken, for the asynchronous algorithm, with proven convergence.

3.1. Approximation quality of the convex underestimator

We now study the quality of the convexified estimator using (4). The quadratic problem was addressed in [5]. We summarize the results here for the reader's convenience and extend them to the L_1 and Huber convex problems.

¹The convex hull of a function γ is its best possible convex underestimator, defined as $\text{conv } \gamma(x) = \sup \{\eta(x) : \eta \leq \gamma, \eta \text{ is convex}\}$. It is hard to determine in general [27].

Table 1: Bounds on the optimality gap for a 1D example.

	True gap $g^* - f^*$	Proposed bound	<i>A priori</i> bound [29]
Quadratic $g_Q^* - f_Q^*$	3.7019	5.5250	11.3405
Absolute value $g_{ \cdot }^* - f_{ \cdot }^*$	1.1416	1.1533	3.0511
Robust Huber $g_R^* - f_R^*$	0.1784	0.1822	0.4786

The optimal value of the cost for any nonconvex g in $\{g_Q, g_{|\cdot|}, g_R\}$, denoted by g^* , is bounded by $f^* = f(x^*) \leq g^* \leq g(x^*)$, where x^* is the minimizer of the convex underestimator f in $\{f_Q, f_{|\cdot|}, f_R\}$, respectively, and $f^* = \min_x f(x)$, is the minimum of function f . A bound for the optimality gap is, thus, $g^* - f^* \leq g(x^*) - f^*$. It is evident that in all cases (quadratic, absolute value, and Huber) f is equal to g when $\|x_i - x_j\| \geq d_{ij}$ and $\|x_i - a_k\| \geq r_{ik}$. When the function terms differ, say, for edges² in a subset $i \sim j \in \mathcal{E}_2 \subset \mathcal{E}$, we necessarily have $(\|x_i - x_j\| - d_{ij})_+ = 0$, leading to³ the bounds $g_Q^* - f_Q^* \leq \sum_{i \sim j \in \mathcal{E}_2} \frac{1}{2} (\|x_i^* - x_j^*\| - d_{ij})^2$ for the quadratic loss, $g_{|\cdot|}^* - f_{|\cdot|}^* \leq \sum_{i \sim j \in \mathcal{E}_2} \frac{1}{2} \|\|x_i^* - x_j^*\| - d_{ij}\|$ for the absolute value loss, and

$$g_R^* - f_R^* \leq \sum_{i \sim j \in \mathcal{E}_2} \frac{1}{2} h_{D_{ij}} (\|x_i^* - x_j^*\| - d_{ij}) \quad (5)$$

for the Huber loss. These bounds are an optimality gap guarantee available after the convexified problem is solved; they tell us how low our estimates can bring the original cost. Our bounds are tighter than the ones available *a priori* from applying [29, Th. 1], which are $g_Q^* - f_Q^* \leq \sum_{i \sim j} \frac{1}{2} d_{ij}^2$ for the quadratic case, $g_{|\cdot|}^* - f_{|\cdot|}^* \leq \sum_{i \sim j} \frac{1}{2} d_{ij}$ for the absolute value problem, and

$$g_R^* - f_R^* \leq \sum_{i \sim j} \frac{1}{2} h_{D_{ij}} (d_{ij}), \quad (6)$$

for the relaxation presented in this paper. We show simulation results for a one-dimensional example averaged over 500 Monte Carlo trials in Table 1. The true average gap $g^* - f^*$ is also listed. In the Monte Carlo trials we obtained a

²The same reasoning applies to anchor terms.

³Note that the minimizers in these expressions are not necessarily identical, but for simplicity we have used a common notation for the three losses.

baseline noisy range measurement as $r_k = \|\|x^* - a_k\| + \nu_k\|$, where x^* is the true position and $\nu_k, k \in \mathcal{A}$ is a zero-mean (i.i.d.) Gaussian random variable with $\sigma = 0.04$. One of the measurements is then corrupted by a zero-mean random variable with $\sigma = 4$, modeling outlier noise. These results show the tightness of the convexified function under such noisy conditions and also demonstrate the looseness of the *a priori* bound in (6). Not only do we use a robust dissimilarity, but we also add a smaller optimality gap by using this particular surrogate. In the end, the Huber-based approximation will be tighter, thus conferring robustness to the estimator, as pointed out by Destino and Abreu [30].

4. Distributed and robust sensor network localization

We construct our algorithm by reformulating (4) as the infimum of a sum of Huber functions composed with a norm, and then by rewriting each of the terms with an alternative representation that uncovers the possibility of a naturally distributed, optimal method for estimating the unknown sensor positions. More specifically, we will (A) reformulate the problem using a novel representation of the Huber function composed with a norm, (B) we will find the closed-form gradient for the new convex cost, and (C) we will verify that this gradient is Lipschitz continuous, minimized over a convex set. The latter is a key prerequisite for deriving a first-order method with optimal convergence rate. For the first step, we invoke that each term of the first summation of (4), corresponding to the edge $i \sim j$, has a variational representation

$$h_{D_{ij}}(\|x_i - x_j\| - d_{ij})_+ = \inf_{\|y_{ij}\| \leq d_{ij}} h_{D_{ij}}(\|x_i - x_j - y_{ij}\|), \quad (7)$$

where $y_{ij} \in \mathbb{R}^p$ is an optimization variable. The result (7) follows from the variational representation⁴ $(\|x_i - x_j\| - d_{ij})_+ = \inf_{\|y\| \leq d_{ij}} \|x_i - x_j - y\|$ already explored in previous work [5] and the fact that the Huber function $h_{D_{ij}}$ is monotonic on the positive argument in \mathbb{R}_+ .

4.1. Alternative representation of the Huber function composed with a norm

Using the variational representation from (7), we can rewrite the convex unconstrained minimization Problem (4) as the constrained problem

$$\underset{x, y, w}{\text{minimize}} \sum_{i \sim j} \frac{1}{2} h_{D_{ij}}(\|x_i - x_j - y_{ij}\|) + \sum_i \sum_{k \in \mathcal{A}_i} \frac{1}{2} h_{R_{ik}}(\|x_i - a_k - w_{ik}\|) \quad (8)$$

subject to $\{\|y_{ij}\| \leq d_{ij}, i \sim j\}, \{\|w_{ik}\| \leq r_{ik}, i \in \mathcal{V}, k \in \mathcal{A}_i\}$,

where we have introduced $y = \{y_{ij} : i \sim j\}$ and $w = \{w_{ik} : i \in \mathcal{V}, k \in \mathcal{A}_i\}$.

We put forward a new representation of the Huber function in (1), when composed with the norm of a vector, $\psi_\delta(u) = h_\delta(\|u\|)$, [in the following proposition](#).

⁴This representation is related to the one used in [31], to describe each one of the nonconvex terms in the ML estimator for Gaussian noise: $(\|x_i - x_j\| - d_{ij})_+ = \inf_{\|y\| = d_{ij}} \|x_i - x_j - y\|$.

Proposition 1 (Representation of the Huber function composed with a norm). *Let $u \in \mathbb{R}^q$, be a vector. Then, the composition of the Huber function with Huber radius δ with the Euclidean norm of u , $\psi_\delta(u) = h_\delta(\|u\|)$ can be written as*

$$\psi_\delta(u) = \|u\|^2 - d_\delta^2(u), \quad (9)$$

where we denote by $d_\delta^2(u)$ the squared Euclidean distance of vector u to a ball of radius δ centered at the origin.

Proof. If the norm of the vector is smaller than the the Huber radius δ , the distance of the vector to the ball centered in the origin with radius δ is zero, and thus we recover the first branch in (1), $h_\delta(\|u\|) = \|u\|^2$ if $\|u\| \leq \delta$. Otherwise, if we have that $\|u\| \geq \delta$, then the squared distance to the disk has a closed form, that is the norm of u minus the radius of the disk, δ . So, the squared distance to the disk is $d_\delta^2(u) = \|u\|^2 - 2\delta\|u\| + \delta^2$. As we are subtracting $d_\delta^2(u)$ to $\|u\|^2$ we obtain the second branch of (1), and, thus, (9). \square

We use this representation to rewrite the cost in problem (8) as

$$\sum_{i \sim j} \frac{1}{2} \psi_{D_{ij}}(x_i - x_j - y_{ij}) + \sum_{i \in \mathcal{V}} \sum_{k \in \mathcal{A}_i} \frac{1}{2} \psi_{R_{ik}}(x_i - a_k - w_{ik}),$$

or, in abbreviated form,

$$\frac{1}{2} \psi_{\mathcal{D}}(Ax - y) + \frac{1}{2} \psi_{\mathcal{R}}(Mx - \alpha - w), \quad (10)$$

where \mathcal{D} is a Cartesian product of balls

$$\mathcal{D} = \prod_{i \sim j} \mathcal{D}_{ij}, \quad \mathcal{D}_{ij} = \{x : \|x\| \leq D_{ij}\}, \quad (11)$$

and similarly for node-anchor terms

$$\mathcal{R} = \prod_{i \in \mathcal{V}, k \in \mathcal{A}_i} \mathcal{R}_{ik}, \quad \mathcal{R}_{ik} = \{x : \|x\| \leq R_{ik}\}. \quad (12)$$

For compactness we have overloaded the notation for ψ in (10); when indexed by a vector of concatenated coordinates and a Cartesian product of balls, it is shorthand for the sum of contributions (9) for each coordinate and for the radius of the ball in the corresponding element of the Cartesian product. The squared distance function indexed by concatenated coordinates and a Cartesian product, $d_{\mathcal{D}}^2(\cdot)$ or $d_{\mathcal{R}}^2(\cdot)$, is also used below and similarly defined in terms of the regular squared distance in (9). Matrix $A = C \otimes I$ in (10) is the Kronecker product of the arc-node incidence matrix⁵ C associated with the graph \mathcal{G} , and

⁵The arc-node incidence matrix C is a $|\mathcal{E}| \times |\mathcal{V}|$ matrix. The rows and the columns of C are indexed by \mathcal{E} and \mathcal{V} , respectively. The (e, i) -entry of C is 0 if node i and edge e are not incident, and otherwise it is 1 or -1 according to the direction agreed on the operation onset by the two nodes involved in edge e .

the identity matrix with dimension of the ambient space (usually, 2 or 3). The product Ax thus concatenates coordinate differences $x_i - x_j$ as required by the ordering of elements chosen for vector y . On the second term of (10) M is a selection matrix that concatenates coordinates x_i according to the ordering of elements chosen for vector w , whereas vector α concatenates anchor coordinates a_k with the same criterion. Consider the aggregation of variables $z = (x, y, w)$; we define the constraint set in (8) as

$$\mathcal{Z} = \{(x, y, w) : \|y_{ij}\| \leq d_{ij}, i \sim j, \|w_{ik}\| \leq r_{ik}, k \in \mathcal{A}_i, i \in \mathcal{V}\}, \quad (13)$$

and the cost as

$$F(z) := \frac{1}{2}\psi_{\mathcal{D}}(Bz) + \frac{1}{2}\psi_{\mathcal{R}}(Ez - \alpha), \quad (14)$$

where $B = [A \quad -I \quad 0]$ and $E = [M \quad 0 \quad -I]$. With this notation, (8) becomes

$$\begin{aligned} & \text{minimize} && F(z) \\ & \text{subject to} && z \in \mathcal{Z}. \end{aligned} \quad (15)$$

Problem (15) is convex and, as we will see next, can be solved by a first-order method with optimal convergence rate, namely, FISTA, proposed by Beck and Teboulle [32]. The required properties for FISTA are: (1) Lipschitz continuous gradient of the cost $F(z)$, (2) known Lipschitz constant, and (3) an easy way to compute the proximal operator of the balls' indicator function, as described in the following sections.

4.2. Gradient

To compute the gradient of the cost in (14), we need the gradient of the squared distance to a convex set — a known result from convex analysis (see [27, Prop. X.3.2.2, Th. X.3.2.3]). Let us denote the squared distance to a convex set C as $\phi(u) = \frac{1}{2}d_C^2(u)$. Then, from convex analysis, we know that ϕ is convex, differentiable, and its gradient is $\nabla\phi(u) = u - P_C(u)$, where $P_C(u)$ is the orthogonal projection of point u onto the set C , $P_C(u) = \operatorname{argmin}_{y \in C} \|u - y\|$. Knowing this, we can compute the gradient of (9) as $\nabla\psi_{\mathcal{R}}(u) = 2u - 2(u - P_{\mathcal{R}}(u)) = 2P_{\mathcal{R}}(u)$, and the gradient of (14) as

$$\nabla F(z) = \frac{1}{2}B^\top \nabla\psi_{\mathcal{D}}(Bz) + \frac{1}{2}E^\top \nabla\psi_{\mathcal{R}}(Ez - \alpha) = B^\top P_{\mathcal{D}}(Bz) + E^\top P_{\mathcal{R}}(Ez - \alpha). \quad (16)$$

Above, to project a vector of concatenated coordinates onto a Cartesian product of balls amounts to concatenating the projection of each coordinate onto the corresponding ball. This is used explicitly in the given summary of the synchronous Algorithm 1.

4.3. Lipschitz constant

Finding a differentiable function such as $F(z)$, whose gradient admits a Lipschitz constant L_F such that

$$\|\nabla F(z_1) - \nabla F(z_2)\| \leq L_F \|z_1 - z_2\|, \text{ for all } z_1, z_2,$$

means that we have access to L_F an upper bound to the curvature of the convex function $F(z)$. The optimal gradient method FISTA [32] can be used once this upper bound is known. We will now obtain such an upper bound L_F with the favourable property that the network can compute it in a distributed way where the complexity per node does not increase as the network grows.

It is widely known that projections onto convex sets shrink distances [33], *i.e.*,

$$\|P_C(u) - P_C(v)\| \leq \|u - v\|. \quad (17)$$

Using this result, we can compute a Lipschitz constant for (16). First, let us focus on the inter-node term in (16):

$$\begin{aligned} \|B^\top P_{\mathcal{D}}(Bu) - B^\top P_{\mathcal{D}}(Bv)\| &\leq \|B\| \|P_{\mathcal{D}}(Bu) - P_{\mathcal{D}}(Bv)\| \\ &\leq \|B\| \|Bu - Bv\| \leq \|B\|^2 \|u - v\| \\ &= \lambda_{\max}(BB^\top) \|u - v\|, \end{aligned}$$

where $\|B\| = \sigma_{\max}(B) = \sqrt{\lambda_{\max}(BB^\top)}$ is the matrix 2-norm of B . The first inequality follows from the Cauchy-Schwarz inequality, the second from (17), and the final one from Cauchy-Schwarz again. The maximum eigenvalue of BB^\top can be bounded by

$$\begin{aligned} \lambda_{\max}(BB^\top) &= \lambda_{\max}\left(\begin{bmatrix} A & -I & 0 \end{bmatrix} \begin{bmatrix} A^\top \\ -I \\ 0 \end{bmatrix}\right) \\ &= \lambda_{\max}(AA^\top + I) \\ &= (1 + \lambda_{\max}(AA^\top)) \\ &= (1 + \lambda_{\max}(L)) \\ &\leq (1 + 2\delta_{\max}), \end{aligned} \quad (18)$$

where L is the graph Laplacian matrix, and δ_{\max} is the maximum node degree of the network⁶. A proof of the inequality $\lambda_{\max} \leq 2\delta_{\max}$ is given in Bapat [34]. In the same way, for the node-anchor terms, we have

$$\|E^\top P_{\mathcal{R}}(Eu) - E^\top P_{\mathcal{R}}(Ev)\| \leq \|E\|^2 \|u - v\| = \lambda_{\max}(EE^\top) \|u - v\|$$

⁶To characterize the network we use the concepts of *node degree* k_i , the number of edges that touch a node v . Maximum node degree is the maximum of this number for all nodes in the network, and *average node degree* $\langle k \rangle = 1/n \sum_{i=1}^n k_i$.

and the constant can be upper-bounded by

$$\begin{aligned}
\lambda_{\max}(EE^\top) &= \lambda_{\max} \left([M0 - I] \begin{bmatrix} M^\top \\ 0 \\ -I \end{bmatrix} \right) \\
&= \lambda_{\max}(MM^\top + I) \\
&\leq (1 + \lambda_{\max}(MM^\top)) \\
&\leq \left(1 + \max_{i \in \mathcal{V}} |\mathcal{A}_i| \right),
\end{aligned} \tag{19}$$

where the last inequality can be deduced from the structure of matrix M : there are identity matrices for each node i for as many anchor measurements it collected. From (18) and (19) we can see that a Lipschitz constant for (14) is

$$L_F = 2 + 2\delta_{\max} + \max_{i \in \mathcal{V}} |\mathcal{A}_i|. \tag{20}$$

We stress that this constant is small, does not depend on the size of the network, and can be computed in a distributed way, for example by flooding [35].

4.4. Synchronous algorithm

The gradient in (16) and its Lipschitz continuity, with the constant in (20), enable us to use Nesterov's optimal gradient method [36, 37], further developed by Beck and Teboulle [32]. Firstly, we must write the problem as an unconstrained minimization using an indicator function $I_{\mathcal{Z}}(u) = \begin{cases} 0 & \text{if } u \in \mathcal{Z} \\ +\infty & \text{otherwise} \end{cases}$, and incorporate the constraints in the problem formulation to obtain the problem $\text{minimize}_z F(z) + I_{\mathcal{Z}}(z)$. Then we perform the proximal minimization of the unconstrained problem using FISTA. For completeness, we outline FISTA, whose optimality convergence proofs can be found in the aforementioned work of Beck and Teboulle [32]. For any initialization $z[0] = z[-1]$ and for $t \geq 1$ the FISTA algorithm performs the following iterations:

$$\begin{aligned}
\zeta &= z[t-1] + \frac{t-2}{t+1}(z[t-1] - z[t-2]), \\
z[t] &= \text{Prox}_{I_{\mathcal{Z}}} \left(\zeta - \frac{1}{L_F} \nabla F(\zeta) \right),
\end{aligned}$$

where $\text{Prox}_{I_{\mathcal{Z}}}(\cdot)$ is the proximal operator of function $I_{\mathcal{Z}}$, that, for the present case, can be computed as

$$\begin{aligned}
\text{Prox}_{I_{\mathcal{Z}}}(z) &= \underset{u}{\text{argmin}} \left(I_{\mathcal{Z}}(u) + \frac{1}{2} \|u - z\|^2 \right) \\
&= P_{\mathcal{Z}}(z),
\end{aligned}$$

where $P_{\mathcal{Z}}(z)$ is the projection of point z onto set \mathcal{Z} . The result for our reformulation is shown in Algorithm 1, where iteration counts are given in square brackets. We denote the entries of ∇F regarding variable x_i as ∇F_i . Each node i will update:

Algorithm 1 Synchronous method: STRONG

Input: $L_F; \{d_{ij}, D_{ij} : i \sim j \in \mathcal{E}\}; \{r_{ik}, R_{i,k} : i \in \mathcal{V}, k \in \mathcal{A}_i\};$ **Output:** \hat{x}

- 1: let $\mathcal{Y}_{ij} = \{y \in \mathbb{R}^p : \|y\| \leq d_{ij}\}$; and $\mathcal{W}_{ik} = \{w \in \mathbb{R}^p : \|w\| \leq r_{ik}\}$;
- 2: each node i chooses and broadcasts arbitrary $x_i[0] = x_i[-1]$;
- 3: set $y_{ij}[0] = P_{\mathcal{Y}_{ij}}(x_i[0] - x_j[0])$; and $w_{ik}[0] = P_{\mathcal{W}_{ik}}(x_i[0] - a_k)$;
- 4: $t = 0$;
- 5: **while** some stopping criterion is not met, each node i **do**
- 6: $t = t + 1$;
- 7: $\xi_i = x_i[t - 1] + \frac{t-2}{t+1}(x_i[t - 1] - x_i[t - 2])$;
- 8: broadcast ξ_i to all neighbors and listen for neighbors' ξ_j ;
- 9: **for** all j in the neighbor set \mathcal{N}_i **do**
- 10: $v_{ij} = y_{ij}[t - 1] + \frac{t-2}{t+1}(y_{ij}[t - 1] - y_{ij}[t - 2])$;
- 11: $y_{ij}[t] = P_{\mathcal{Y}_{ij}}\left(v_{ij} + \frac{1}{L_F}P_{\mathcal{D}_{ij}}(\xi_i - \xi_j - v_{ij})\right)$;
- 12: **end for**
- 13: **for** all k in the anchor set \mathcal{A}_i **do**
- 14: $\omega_{ik} = w_{ik}[t - 1] + \frac{t-2}{t+1}(w_{ik}[t - 1] - w_{ik}[t - 2])$;
- 15: $w_{ik}[t] = P_{\mathcal{W}_{ik}}\left(\omega_{ik} + \frac{1}{L_F}P_{\mathcal{R}_{ik}}(\xi_i - a_k - \omega_{ik})\right)$;
- 16: **end for**
- 17: $\nabla F_i = \sum_{j \in \mathcal{N}_i} P_{\mathcal{D}_{ij}}(\xi_i - \xi_j - v_{ij}) + \sum_{k \in \mathcal{A}_i} P_{\mathcal{R}_{ik}}(\xi_i - a_k - \omega_{ik})$;
- 18: $x_i[t] = \xi_i - \frac{1}{L_F}\nabla F_i$;
- 19: **end while**
- 20: **return** $\hat{x}_i = x_i[t]$

- the current estimate of its own position,
- each one of the y_{ij} for all the incident edges, and
- the anchor terms w_{ik} , if any.

In step 7 we have the extrapolation step for each x_i , whereas in steps 10 and 14 we can see the update of the extrapolation steps for each one of the edge variables y_{ij} , and w_{ik} , respectively. In terms of computational complexity at each node, the operations are multiplications and summations, and thus do not demand intensive calculus and the corresponding battery drain. The same applies to the nonconvex Huber method [19]. In the other extreme, the SDP method [26] is addressed with interior point algorithms, that are cubic in the problem dimension.

Paralellizability. We observe that each block of $z = (x, y, w)$ at iteration t only needs local neighborhood information, as shown in Algorithm 1. To demonstrate the natural distribution of the method we go back to (16). Here, the term $E^\top P_{\mathcal{R}}(Ez - a)$ only involves anchor measurements relative to each node, and so it is distributed. The term $B^\top P_{\mathcal{D}}(Bz)$ is less clear. The vector Bz collects $x_i - x_j - y_{ij}$ for all edges $i \sim j$ and to it we apply the projection operator

onto the Cartesian product of balls. This is the same as applying a projection of each edge onto each ball. When left multiplying with B^\top we get $B^\top P_{\mathcal{D}}(Bz)$. The left multiplication by B^\top will group at the position of each node variable x_i the contributions of all incident edges to node i .

Edge variables. Recall that we introduced edge variables y_{ij} in (7) to reformulate terms in the maximum-likelihood function in a more tractable form. These are associated with edges linking pairs of nodes in the measurement graph \mathcal{G} . Variables w_{ik} play the same role for node-anchor terms. To update the y_{ij} variables we could designate one of the incident nodes, i or j , as responsible for the update and then communicate the result to the non-computing neighbor. But, to avoid this expensive extra communication, we decide that each node i should compute its own y_{ij} , where $y_{ij} = -y_{ji}$ for all edges. Also, with this device, the gradient entry regarding variable x_i would be $\sum_{j \in \mathcal{N}_i} C_{(i \sim j, i)} P_{\mathcal{D}_{ij}}(C_{(i \sim j, i)}(x_i - x_j - y_{ij}))$. The symbol $C_{(i \sim j, i)}$ denotes the arc-node incidence matrix entry relative to edge $i \sim j$ (row index) and node i (column index). As the projection onto a ball \mathcal{B} of radius δ centered at the origin can be written as

$$P_{\mathcal{B}}(u) = \begin{cases} \frac{u}{\|u\|} \delta & \text{if } \|u\| > \delta \\ u & \text{if } \|u\| \leq \delta \end{cases},$$

then $P_{\mathcal{B}}(-u) = -P_{\mathcal{B}}(u)$, and, thus, the gradient entry regarding variable x_i becomes $\sum_{j \in \mathcal{N}_i} P_{\mathcal{D}_{ij}}(x_i - x_j - y_{ij})$, as stated in Algorithm 1.

Communications. For each iteration t , the algorithm requires only that each agent i broadcast to its neighbors one vector in the ambient space (\mathbb{R}^2 or \mathbb{R}^3) with the Nesterov extrapolated point ξ_i . The position estimates $x_i[t]$, node-anchor variables $w_{ik}[t]$, and edge variables $y_{ij}[t]$ are computed internally at each node.

4.5. Asynchronous algorithm

In Section 4.4 we presented a distributed method addressing the robust network localization problem in a scalable manner, where each node uses information from its neighborhood and performs a set of simple arithmetic computations. But the results still depend critically on synchronous computation, where nodes progress in lockstep through iterations. As the number of processing nodes becomes very large, this synchronization can become seriously difficult — and unproductive. An asynchronous approach is called for in such very large-scale and faulty settings. In an asynchronous time model, the nodes move forward independently and algorithms should withstand certain types of faults, like temporary unavailability of a node. To address this issue, we present a fully asynchronous method, based on a broadcast gossip scheme (c.f. Shah [38] for an extended survey of gossip algorithms).

Nodes are equipped with independent clocks ticking at random times (say, as Poisson point processes). When node i 's clock ticks, it performs the update

Algorithm 2 Asynchronous method: asyncSTRONG

Input: $L_F; \{d_{ij}, D_{ij} : i \sim j \in \mathcal{E}\}; \{r_{ik}, R_{i,k} : i \in \mathcal{V}, k \in \mathcal{A}_i\};$
Output: \hat{x}

- 1: let $\mathcal{Y}_{ij} = \{y \in \mathbb{R}^p : \|y\| \leq d_{ij}\}$; and $\mathcal{W}_{ik} = \{w \in \mathbb{R}^p : \|w\| \leq r_{ik}\}$;
 - 2: each node i chooses and broadcasts random $x_i[0]$;
 - 3: **Initialization:** set $y_{ij}[0] = P_{\mathcal{Y}_{ij}}(x_i[0] - x_j[0])$; and $w_{ik}[0] = P_{\mathcal{W}_{ik}}(x_i[0] - a_k)$;
 - 4: $t = 0$;
 - 5: **while** some stopping criterion is not met, each node i **do**
 - 6: $t = t + 1$;
 - 7: $x_i[t] = \begin{cases} \underset{\substack{\xi_i, \{y_{ij} \in \mathcal{Y}_{ij}, j \in \mathcal{N}_i\}, \\ \{w_{ik} \in \mathcal{W}_{ik}, k \in \mathcal{A}_i\}}}{\text{argmin}} F_i(\xi_i, \{y_{ij}\}, \{w_{ik}\}) & \text{if } \chi_t = i \\ x_i[t-1] & \text{otherwise;} \end{cases}$
 - 8: if $\chi_t = i$, broadcast $x_i[t]$ to neighbors
 - 9: **end while**
 - 10: **return** $\hat{x} = x[t]$
-

of its variables and broadcasts the update to its neighbors. Let the order of node activation be collected in $\{\chi_t\}_{t \in \mathbb{N}}$, a sequence of independent random variables taking values on the set \mathcal{V} , such that the probability $\mathbb{P}(\chi_t = i)$ is always positive, i.e.,

$$\mathbb{P}(\chi_t = i) = P_i > 0. \quad (21)$$

This assumption ensures that the node can be activated. The asynchronous update of variables on node i is summarized in Algorithm 2 and described in detail below. It is useful to recast Problem (14)–(15) as

$$\begin{aligned} \underset{x, y, w}{\text{minimize}} \sum_i \left(\sum_{j \in \mathcal{N}_i} \frac{1}{4} \|x_i - x_j - y_{ij}\|^2 - \frac{1}{4} d_{\mathcal{D}_{ij}}^2(x_i - x_j - y_{ij}) + \right. \\ \left. \sum_{k \in \mathcal{A}_i} \frac{1}{2} \|x_i - a_k - w_{ik}\|^2 - \frac{1}{2} d_{\mathcal{R}_{ik}}^2(x_i - a_k - w_{ik}) \right) \\ \text{subject to} \quad \|y_{ij}\| \leq d_{ij}, \quad \|w_{ik}\| \leq r_{ik}, \end{aligned} \quad (22)$$

where the factor $\frac{1}{4}$ accounts for the duplicate terms when considering summations over nodes instead of over edges. Our strategy for obtaining an asynchronous algorithm simply consists in solving a single-source localization problem at any given node upon wake-up, fixing the neighbor positions to their last known values. Node i thus solves

$$\begin{aligned} \underset{\substack{x_i, \{y_{ij} : j \in \mathcal{N}_i\}, \\ \{w_{ik} : k \in \mathcal{A}_i\}}}{\text{minimize}} F_i(x_i, \{y_{ij}\}, \{w_{ik}\}) \\ \text{subject to} \quad \|y_{ij}\| \leq d_{ij}, \quad \|w_{ik}\| \leq r_{ik}, \end{aligned} \quad (23)$$

where

$$F_i(x_i, \{y_{ij}\}, \{w_{ik}\}) := \sum_{j \in \mathcal{N}_i} \frac{1}{4} \psi_{D_{ij}}(x_i - x_j - y_{ij}) + \sum_{k \in \mathcal{A}_i} \frac{1}{2} \psi_{R_{ik}}(x_i - a_k - w_{ik}).$$

Problem (23) is convex, solvable at each node by a general purpose solver. Nevertheless, that approach would not take advantage of the specific problem structure, thus depriving the solution of an efficient and simpler computational procedure. Again, Problem (23) can be solved by the Nesterov optimal first-order method, because the gradient of F_i is Lipschitz continuous in x_i, y_{ij} , and w_{ik} , accepting the same Lipschitz constant as F , in (20).

Communications. For each iteration t , the algorithm requires only that the agent $i = \chi_t$ broadcast to its neighbors a vector in the ambient space (\mathbb{R}^2 or \mathbb{R}^3) with the position estimate $x_i[t]$.

5. Convergence analysis

In this section we address the convergence of Algorithms 1 and 2. We provide convergence guarantees and rate of convergence for the synchronous version, and we also prove convergence for the asynchronous method.

5.1. Synchronous algorithm

As shown in Section 4, Problem (15) is convex and the cost function has a Lipschitz continuous gradient. As proven by Nesterov [36, 37], and further developed by Beck and Teboulle [32], Algorithm 1 converges at the optimal rate $O(t^{-2})$. Specifically, $F(z^t) - F^* \leq \frac{2L_F}{(t+1)^2} \|z^0 - z^*\|^2$, where F^* is the optimal value and z^* is a minimizer of Problem (15).

5.2. Asynchronous algorithm

To investigate the convergence of Algorithm 2, as it is a constrained problem unlike [5], we will use a totally different proof strategy, not by crafting a supermartingale that bounds the gradient norm, but depending on the Borel-Cantelli Lemma, as formally described in Appendix A. We need the following trivial assumption for the network localization problem:

Assumption 2. *The graph \mathcal{G} is connected, and there is at least one node in \mathcal{G} with an anchor measurement.*

This assumption is naturally fulfilled: if the network is supporting several disconnected components, then each can be treated as a different network, and, for disambiguation, range-based, static localization requires the availability of 3 anchors in 2D and 4 anchors in 3D. The convergence of Algorithm 2 is stated next.

Theorem 3 (Almost sure convergence). *Let Assumption 2 hold. Consider Problem (15), and the sequence $\{z^t\}_{t \in \mathbb{N}}$ generated by Algorithm 2. Define the solution set as $\mathcal{Z}^* = \{z \in \mathcal{Z} : F(z) = F^*\}$. Then*

1. $d_{\mathcal{Z}^*}(z^t) \rightarrow 0$, a.s.;
2. $F(z^t) \rightarrow F^*$, a.s.

We stress that the convergence stated in this result is the strongest possible, encompassing convergence in expectation, *i.e.*, the expected value of iterates converge to a minimizer, and convergence in probability, where the probability density function of the iterates converges to the true probability density function of a minimizer. Moreover, we prove that the iterates of our algorithm converge to a minimizer of our function with probability one.

Next, we will state in Theorem 4 that, with probability one, Algorithm 2 converges in a *finite* number of iterations, for a given precision. Both proofs can be found in Appendix A.

Theorem 4. *For a prescribed precision ϵ , the sequence of iterates $\{z^t\}_{t \in \mathbb{N}}$ converges in K_ϵ iterations. The expected count is*

$$\mathbb{E}[K_\epsilon] \leq \frac{F(z^0) - F^*}{b_\epsilon}, \quad (24)$$

where b_ϵ is a constant that depends on the specified ϵ .

In practice, this result states that the number of iterations until convergence will be a finite number, and not infinity, *e.g.*, as in typical distributed consensus algorithms.

6. Numerical experiments

The experimental setup consists in a uniquely localizable geometric network deployed in a square area with side of 1 Km, with four anchors located at the corners, and ten sensors. The average node degree of the network is 4.3. The regular noisy range measurements are generated according to $d_{ij} = \|x_i^* - x_j^*\| + \nu_{ij}$, and $r_{ik} = \|x_i^* - a_k\| + \nu_{ik}$, where x_i^* is the true position of node i , and $\{\nu_{ij} : i \sim j \in \mathcal{E}\} \cup \{\nu_{ik} : i \in \mathcal{V}, k \in \mathcal{A}_i\}$ are independent Gaussian random variables with zero mean and standard deviation 40 m. Node 7 is malfunctioning and with some probability all measurements related to it are corrupted by noise with heavy-tailed distributions with a scale parameter of 4 Km, unless stated otherwise. Two families of heavy-tailed distributions were used: Laplace and Cauchy. The Laplace distribution is well-known for modeling outlier noise [39], and Cauchy noise is frequent in contexts like radar echo, atmospheric noise, and underwater acoustic signals noise [40].

Node 8 is badly calibrated, so measurements are 20% of the true value, which is also affected by white noise with the same standard deviation of 40 m. We

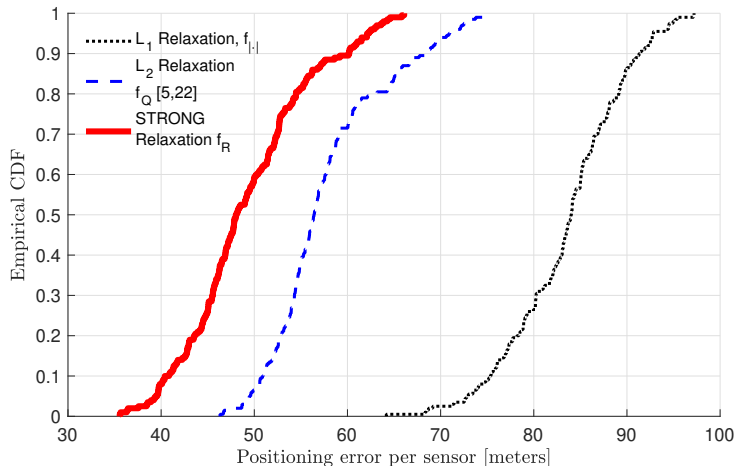


Figure 2: Underestimator performance: Empirical CDF for the positioning error per sensor, in meters. Our Huber-based relaxation shows higher accuracy than the L_2 and the robust L_1 relaxations, in an experiment where 2 nodes in 10 are affected by Laplacian noise.

sampled both regular and outlier noise. The performance metric used to assess accuracy is the positioning error per sensor, defined as

$$\epsilon(m) = \frac{\|\hat{x}(m) - x^*\|}{|\mathcal{V}|}, \quad (25)$$

where $\hat{x}(m)$ denotes the position estimates for all sensors in Monte Carlo trial m . The average positioning error is defined as

$$\epsilon = \frac{1}{M} \sum_{m=1}^M \epsilon(m),$$

where M is the number of Monte Carlo trials.

6.1. Underestimator performance

The convex optimization problems were solved with `cvx` [41]. We ran 200 Monte Carlo trials, where we sampled the measurement and outlier noise sources. The empirical CDFs of estimation errors are shown in Figure 2, which demonstrate that the Huber robust cost used in STRONG can reduce the error per sensor by more than 30 meters, when compared with the L_1 discrepancy, and about 10 m for the L_2 discrepancy. The sensitivity to the value of the Huber parameter R in (1) is small in the range from 40 to 100 m. In fact, for this range, the positioning error variation per sensor is about 10 cm. The proposed estimator exhibits smaller error per sensor than the competing algorithms for all tested values of the parameter. We observe that the error increases when R approaches the standard deviation of the regular Gaussian noise, meaning that

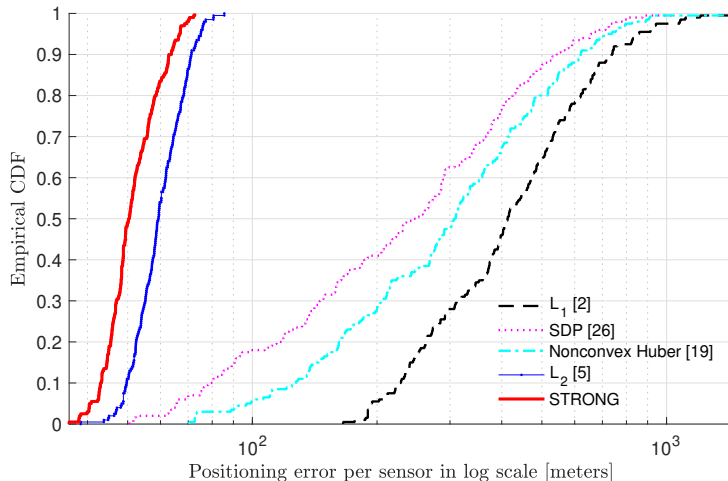


Figure 3: Accuracy of the distributed synchronous algorithm. Empirical CDF for the positioning error per sensor, in meters, for the outlier experiment, with Laplacian noise. Our STRONG algorithm outperforms all tested methods, including the nonconvex Huber [19], and the L_2 [5]. Note that although L_2 seems to have a close performance at the scale of the plot, the accuracy gain of STRONG is still large.

the Huber loss gets closer to the L_1 loss and, thus, is no longer adapted to regular noise ($R = 0$ corresponds exactly to the L_1 loss); in the same way, as R increases, so does the extent of the quadratic section, and the estimator gets less robust to outliers, so, again, the error increases.

6.2. Performance of the distributed synchronous Algorithm 1

We tested Algorithm 1 using the same setup as in the previous section, running 200 Monte Carlo trials. We benchmark our method comparing with the performance of the centralized solutions in Oğuz-Ekim *et al.*, [2], the SDP presented by Simonetto and Leus⁷ [26], and also the distributed locally convergent algorithm by Korkmaz and Van der Veen⁸ [19]. The results are summarized in Figures 3, for Laplacian noise, and 4 for Cauchy noise. The empirical CDFs for positioning error (25) indicate that the STRONG algorithm has the highest accuracy among the tested methods. As depicted in Figures 3 for Laplace and 4 for Cauchy noise, it is noticeable that the STRONG algorithm outperforms in accuracy the algorithm in [5] for the quadratic discrepancy by more than 14 meters per sensor in average positioning error. When we compare to a L_1 -

⁷In [26], the authors present a distributed ESDP algorithm which is a relaxation of the centralized SDP. As the simulation time for the distributed, edge-based algorithm is considerable we benchmarked against the tighter and more accurate centralized SDP solution.

⁸This distributed method directly minimizes the nonconvex cost (3), thus delivering a local solution, that depends on the initialization point. The algorithm was initialized with samples of a zero mean Gaussian distribution.

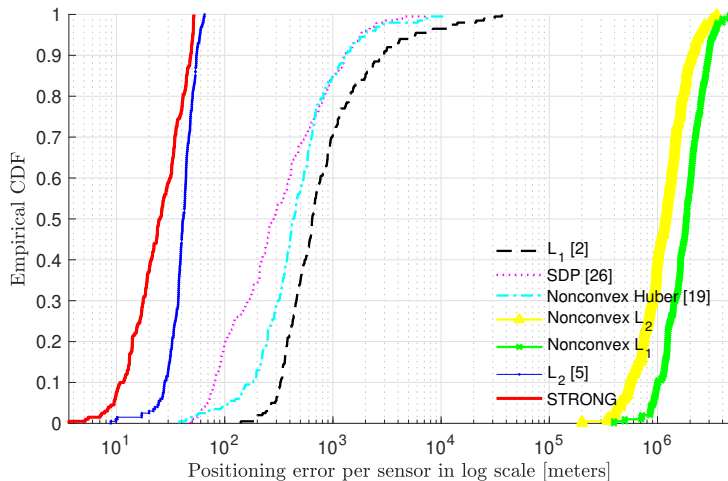


Figure 4: Accuracy of the distributed synchronous algorithm. Empirical CDF for the positioning error per sensor, in meters, for the outlier experiment, with Cauchy noise. Our STRONG algorithm still outperforms all other methods.

type algorithm — in this case the L_1 relaxation from Oğuz-Ekim *et al.* [2] — under the same conditions, the improvement of performance of our solution is, on average, about 120 meters per sensor. We also tested all methods regarding the probability of having a malfunctioning (or malicious) node in the network, injecting both multiplicative and Laplacian noise in Figure 6 and Cauchy noise in Figure 5 into the estimation process. From the positioning error obtained in our simulations we see that outlier probability for the two heavy-tailed noise schemes drives the performance of the algorithms. We can also conclude that, for the tested scenarios, STRONG maintains consistently the lowest mean positioning error.

We have experimented with the Gaussian measurement noise power, but, in the presence of outliers and for the same outlier probability, the influence of varying the power of the measurement noise is negligible, compared with the effect of outlier noise.

6.3. Performance of the distributed asynchronous Algorithm 2

Here, we tested Algorithm 2, async STRONG, using Gaussian outlier noise with a standard deviation of 5 Km. We benchmarked it against the synchronous Algorithm 1, STRONG, since both minimize the same cost function. The algorithms were allowed to run with the same communication load, and the mean positioning error for the considered measurement noise levels (excluding outlier noise) is depicted in Figure 7. We can observe that the async STRONG algorithm fares better than STRONG for the same level of communication. This is an interesting phenomenon that has already been empirically observed in several optimization algorithms when comparing deterministic and randomized

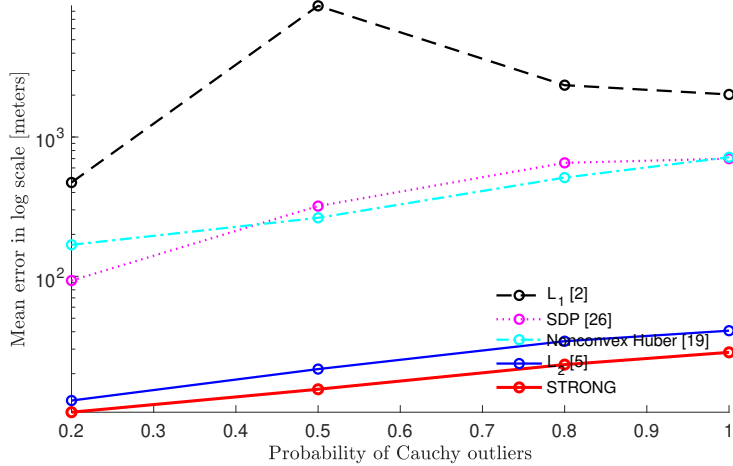


Figure 5: As the probability of having one malfunctioning node injecting Cauchy outlier measurements into the distributed estimation process increases, all the methods increase the positioning error, as expected. The proposed STRONG method has the lowest mean error for 200 random trials for each value of the outlier probability.

versions. In fact, Bertsekas and Tsitsiklis [42, Section 6.3.5] provide a proof of this behavior for a restricted class of algorithms. Figure 8 further explores the numerical results, by examining the CDF of the positioning error for the tested Monte Carlo trials. Here we see the superior accuracy of the asynchronous Huber Algorithm 2, for the same communications volume. We must, nevertheless, emphasize that this result does not correspond to a faster algorithm, in terms of running time: STRONG in one iteration updates all of the node positions in parallel, and broadcasts the current estimates across neighbors, whereas in async STRONG only one node operates at a time. As the wireless medium might be much more intensively used for synchronous updates than for random gossip interactions, it seems entirely possible that for the same operation time STRONG will outperform async STRONG — at the expense of greater overall power consumption.

7. Discussion and conclusions

We presented two distributed, fast, and robust localization algorithms that take noisy ranges and a few anchor locations, and output accurate estimates of the node positions. We approximated the difficult nonconvex problem based on the Huber discrepancy in (2) with a convex envelope of terms, robust to outliers. How does the Huber-based approximation in (4) compare to similar L_1 and L_2 underestimators, frequently used in robust estimation? A smaller optimality gap means a more robust approximation [30]: We designed a bound that certifies the gap between the nonconvex and surrogate optimal values for Huber, L_1 and L_2 , which shows a tighter gap in the Huber case. A numerical

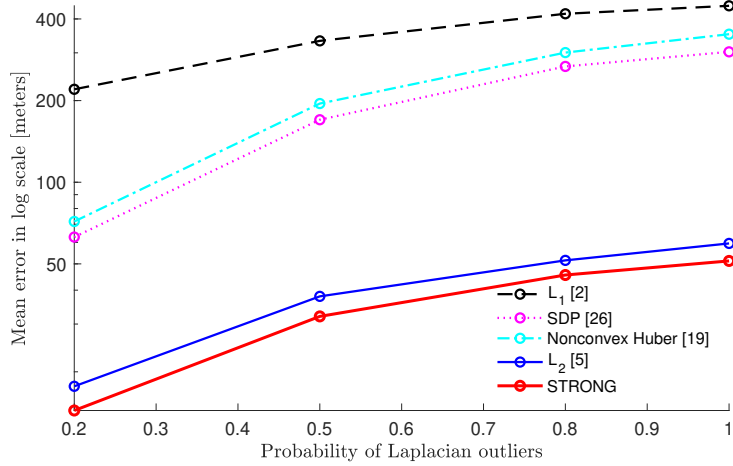


Figure 6: As with Cauchy noise in Figure 5, The error response of the tested methods increases with the probability of multiplicative and Laplace noise.

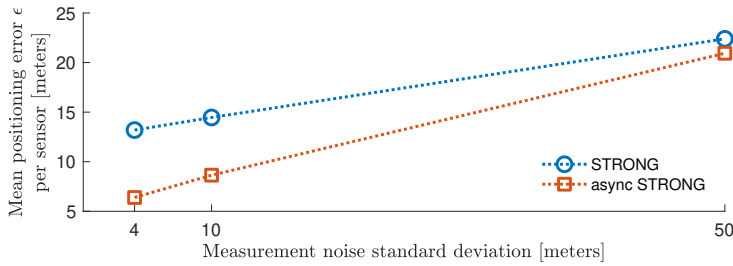


Figure 7: Mean positioning error for different noise standard deviations.

analysis of a star network in 1D unveiled that the optimality gap for the Huber approximation was one order of magnitude smaller than the quadratic or absolute value convexified problems, with respect to their nonconvex counterparts. Numerical network localization trials verify the robust behavior of this surrogate under different types of outlier noise. In order to develop a distributed method we needed to transform our cost. So, we proposed a new representation of the Huber function composed with a norm, and arrived at a novel distributed gradient method, STRONG, with optimal convergence rate. But our STRONG algorithm requires synchronization of nodes, which may be inconvenient in many applications. Thus, we put forward a novel asynchronous method for robust network localization, async STRONG, which converges with probability one. Like other relaxation methods, ours are prone to the anchor convex hull problem: preliminary results show that the positioning accuracy degrades — albeit graciously — when node positions depart from the convex hull of the anchors. Arguably, this is not a big issue because engineers in general can control the choice or placement of anchors, and can delimit the area under

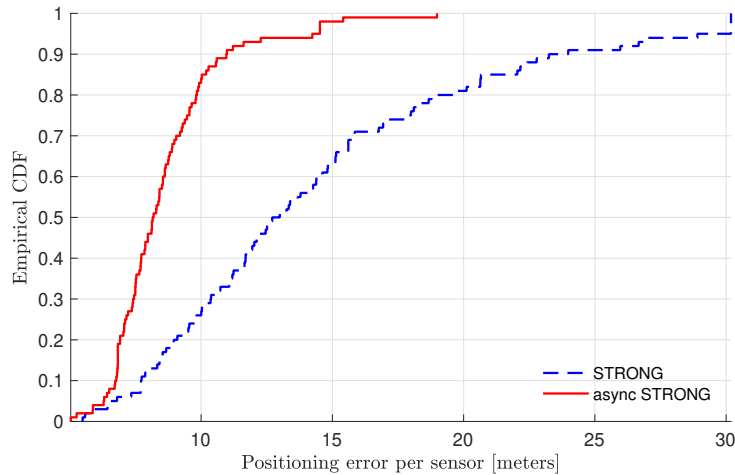


Figure 8: Accuracy of the distributed asynchronous algorithm: positioning error of synchronous algorithm 1 versus asynchronous algorithm 2. CDF of the positioning error. Noise standard deviation of 10 meters (corresponding to the second data point in Fig. 7). Both algorithms were run with the same communication load. Experiment within a square with 1 Km sides.

survey.

In summary, both our algorithms work with simple computations at each node and minimal communication requirements, have provable convergence, and show superior performance in our numerical experiments.

Acknowledgment

The authors would like to thank Prof. Pinar Oğuz-Ekim and Dr. Andrea Simonetto for providing the MATLAB implementations of their published algorithms. Also, we thank Prof. João Xavier for insightful discussions during this research.

This research was partially supported by Fundação para a Ciência e a Tecnologia (projects HARMONY PTDC/EEL-AUT/31411/2017, and LARSyS - FCT Plurianual funding 2020-2023).

Appendix A. Proofs of Theorems 3 and 4

Appendix A.1. Definitions

First, we review the definition of a block optimal point and describe some useful mathematical objects used in the proofs.

Definition 5. A point $z^\bullet = (z_i^\bullet)_{i \in \mathcal{V}}$ is block optimal for the constrained function F in (14) if, for all i , $z_i^\bullet = (x_i^\bullet, \{y_{ij}^\bullet\}, \{w_{ik}^\bullet\})$ is a minimizer of the restricted function F_i defined in (23) [43].

We denote the sublevel sets of F as $T_\alpha = \{z : F(z) \leq \alpha\}$ and the minimum of that function as F^* . We also define the sets

$$\mathcal{Z}^* = T_{F^*} \cap \mathcal{Z} \quad (\text{A.1})$$

$$\mathcal{Z}_\epsilon = \{z \in \mathcal{Z} : d_{\mathcal{Z}^*}(z) < \epsilon\} \quad (\text{A.2})$$

$$\mathcal{Z}_\epsilon^c = \{z \in \mathcal{Z} : d_{\mathcal{Z}^*}(z) \geq \epsilon\} \quad (\text{A.3})$$

$$\hat{\mathcal{Z}}_\epsilon^c = \mathcal{Z}_\epsilon^c \cap T_{F(z^0)}, \quad (\text{A.4})$$

where $\hat{\mathcal{Z}}_\epsilon^c$ is the set of all points in \mathcal{Z} whose distance to the optimal set \mathcal{Z}^* is larger than ϵ , but also belong to the initial sublevel set of F . We will see that the iterates of Algorithm 2 belong to $\hat{\mathcal{Z}}_\epsilon^c$ until they reach the absorbing set \mathcal{Z}_ϵ . We also define the *expected improvement function* as

$$\rho(z) = \mathbb{E}[F(Z(k+1)) | Z(k) = z] - F(z). \quad (\text{A.5})$$

It is easy to see that the expected improvement ρ can also be written as

$$\rho(z) = \sum_{i=1}^n (F_i^*(z) - F(z)) P_i, \quad (\text{A.6})$$

where $F_i^*(z)$ denotes the minimum of F_i in (23) over its restricted argument for the current iterate z , and P_i is the probability of the event “node i is awoken at time t ” (we recall the independence of the random variables χ_t defined in (21)). For notational convenience, we introduce the function

$$\varphi(z) = -\rho(z), \quad (\text{A.7})$$

which, by construction of Algorithm 2, is always non-negative.

Appendix A.1.1. Auxiliary Lemmas

The analysis is founded on Lemma 7, where the symmetric of the expected improvement is shown to attain a positive infimum on the set $\hat{\mathcal{Z}}_\epsilon^c$. Lemma 6 will be instrumental in the proof of Lemma 7 but contains also some useful properties of function F and the solution set \mathcal{Z}^* .

Lemma 6 (Basic properties). *Let F be defined as in (14). Then the following properties hold.*

1. F is coercive;
2. $F^* \geq 0$ and $\mathcal{Z}^* \neq \emptyset$;
3. \mathcal{Z}^* is compact;
4. If z^\bullet is block optimal for F in \mathcal{Z} , then it is a global minimizer for F in \mathcal{Z} .

- Proof.* 1. By Assumption 2 in Section 5.2 there is a path from each node i to some node j which is connected to an anchor k . Also, we know that, by definition, $\|y_{ij}\|$ and $\|w_{ik}\|$ are bounded by the ranges $d_{ij} < \infty$ and $r_{ik} < \infty$. So these components of z will have no effect in the limiting behavior of F . If $\|x_i\| \rightarrow \infty$ there are two cases: (1) there is at least one edge $t \sim u$ along the path from i to j where $\|x_t\| \rightarrow \infty$ and $\|x_u\| \not\rightarrow \infty$, and so $h_{R_{tu}}(\|x_t - x_u - y_{tu}\|) \rightarrow \infty$; (2) if $\|x_u\| \rightarrow \infty$ for all u in the path between i and j , in particular we have $\|x_j\| \rightarrow \infty$ and so $h_{R_{ajk}}(\|x_j - a_k - w_{jk}\|) \rightarrow \infty$, and in both cases $F \rightarrow \infty$. Thus, F is coercive.
2. F defined in (14) is a continuous, convex and real valued function lower bounded by zero; so, the infimum F^* exists and is non-negative. To prove that this infimum is attained and $\mathcal{Z}^* \neq \emptyset$, we observe that the set \mathcal{Z} is a cartesian product of the closed sets \mathbb{R}^{np} , $\{y \in \mathbb{R}^{|\mathcal{E}|p} : y = \{y_{ij}, \|y_{ij}\| \leq d_{ij}, i \sim j \in \mathcal{E}\}\}$, and $\{w \in \mathbb{R}^{\sum_i |\mathcal{A}_i|p} : w = \{w_{ik}, \|w_{ik}\| \leq r_{ik}, i \in \mathcal{V}, k \in \mathcal{A}_i\}\}$, and thus \mathcal{Z} is also closed. Now consider a sublevel set T_α , which is compact because F is coercive. For some α , the intersection of T_α and \mathcal{Z} is nonempty and it is known that the intersection of a closed and a compact set is compact [44, Corollary to 2.35], so $T_\alpha \cap \mathcal{Z}$ is compact. As function F is convex, it is also continuous on the compact set $T_\alpha \cap \mathcal{Z}$ and, by the extreme value theorem, the value $p = \inf_{z \in T_\alpha \cap \mathcal{Z}} F(z)$ is attained. It is obvious that $\inf_{z \in T_\alpha \cap \mathcal{Z}} F(z) = \inf_{z \in \mathcal{Z}} F(z)$.
3. $\mathcal{Z}^* = T_\alpha \cap \mathcal{Z}$ for $\alpha = F^*$, and we established in the previous proof that $T_\alpha \cap \mathcal{Z}$ is compact.
4. If z^\bullet is block-optimal, then $\langle \nabla F_i(z_i^\bullet), z_i - z_i^\bullet \rangle \geq 0$ for all i . When stacking the inequalities for all i , we get $\langle \nabla F(z^\bullet), z - z^\bullet \rangle \geq 0$, which proves the claim. \square

Lemma 7. *Let φ be defined as in (A.7), taking values on the set $\hat{\mathcal{Z}}_\epsilon^c$ in (A.4). Then,*

1. *Function φ is positive:*

$$\varphi(z) > 0, \quad \text{for all } z \in \hat{\mathcal{Z}}_\epsilon^c; \quad (\text{A.8})$$

2. *As a consequence, function φ is bounded below by a finite positive value a_ϵ :*

$$\inf_{z \in \hat{\mathcal{Z}}_\epsilon^c} \varphi(z) = a_\epsilon. \quad (\text{A.9})$$

Proof. We start by proving the first claim, $\varphi(z) > 0$ for all $z \in \hat{\mathcal{Z}}_\epsilon^c$. Suppose $\varphi(z) = 0$; then, by Equation (A.6) $F^i(z) = F(z)$, which means that z is block optimal. By Lemma 6, z is also global optimal, which contradicts the fact that z belongs to the set $\hat{\mathcal{Z}}_\epsilon^c$. The second claim follows by observing that φ is a sum of real valued functions and, thus, a real valued function, and that $\varphi(z)$ is bounded below by zero in $\hat{\mathcal{Z}}_\epsilon^c$ and so it has a positive infimum for $\hat{\mathcal{Z}}_\epsilon^c$. \square

Appendix A.1.2. Theorems

Equipped with the previous Lemmas, we are now ready to prove the Theorems stated in Section 5.2.

Proof of Theorem 3. We denote the random variable corresponding to the outcome of the t -th loop step of Algorithm 2 as Z^t . The expected value of the expected improvement function ρ (A.5) is

$$\begin{aligned}\mathbb{E}[\rho(Z^t)] &= \mathbb{E}[\mathbb{E}[F(Z^{t+1}) | Z^t]] - \mathbb{E}[F(Z^t)] \\ &= \mathbb{E}[F(Z^{t+1})] - \mathbb{E}[F(Z^t)],\end{aligned}$$

where the second equality comes from the tower property documented, *e.g.*, in Williams [45]. This expectation can also be written as

$$\begin{aligned}\mathbb{E}[\rho(Z^t)] &= \mathbb{E}[\rho(Z^t) | Z^t \in \hat{Z}_\epsilon^c] \mathbb{P}(Z^t \in \hat{Z}_\epsilon^c) + \mathbb{E}[\rho(Z^t) | Z^t \notin \hat{Z}_\epsilon^c] \mathbb{P}(Z^t \notin \hat{Z}_\epsilon^c) \\ &\leq \mathbb{E}[\rho(Z^t) | Z^t \in \hat{Z}_\epsilon^c] \mathbb{P}(Z^t \in \hat{Z}_\epsilon^c).\end{aligned}$$

By combining both we get

$$\mathbb{E}[F(Z^{t+1})] - \mathbb{E}[F(Z^t)] \leq \mathbb{E}[\rho(Z^t) | Z^t \in \hat{Z}_\epsilon^c] \mathbb{P}(Z^t \in \hat{Z}_\epsilon^c)$$

which can be further bounded using Lemma 7 as

$$\mathbb{E}[F(Z^{t+1})] - \mathbb{E}[F(Z^t)] \leq -a_\epsilon p_t$$

where $p_t = \mathbb{P}(Z^t \in \hat{Z}_\epsilon^c)$. By expanding the recursion we obtain

$$\mathbb{E}[F(Z^{t+1})] \leq -a_\epsilon \sum_{k=1}^t p_k + F(z^0),$$

which provides a bound on the sum of probabilities p_k when rearranged as

$$\sum_{k=1}^t p_k \leq \frac{F(z^0) - \mathbb{E}[F(Z^{t+1})]}{a_\epsilon}.$$

Taking t up to infinity, we obtain

$$\begin{aligned}\sum_{k=1}^{\infty} p_k &\leq \frac{F(z^0) - \mathbb{E}[F(Z^\infty)]}{a_\epsilon} \\ &\leq \frac{F(z^0) - F^*}{a_\epsilon}.\end{aligned}$$

This means that the infinite series of probabilities p_k takes on a finite value; by the Borel-Cantelli Lemma, we get $\mathbb{P}(Z^t \in \hat{Z}_\epsilon^c, \text{ i.o.}) = 0$, where *i.o.* stands for *infinitely often*. This concludes the proof, since this statement is equivalent to the first claim of Theorem 3. \square

Proof of Theorem 4. We consider a variant of the set defined in (A.2)

$$\mathcal{Y}_\epsilon = T_{F^*+\epsilon} \cap \mathcal{Z},$$

and, similarly to (A.3)–(A.4), its complement in \mathcal{Z} , \mathcal{Y}_ϵ^c , and the intersection with the initial sublevel set, $\hat{\mathcal{Y}}_\epsilon^c = \mathcal{Y}_\epsilon^c \cap T_{F(z^0)}$. Using the same arguments as in Lemma 7, we can prove that $\inf_{z \in \hat{\mathcal{Y}}_\epsilon^c} \varphi(z) = b_\epsilon$, $0 < b_\epsilon < \infty$. We now define a sequence of points \tilde{z}^t such that

$$\tilde{z}^t = \begin{cases} z^t & \text{if } z^t \in \hat{\mathcal{Y}}_\epsilon^c \\ z^* & \text{otherwise,} \end{cases}$$

and the sequence of real values $\rho(\tilde{z}^t) = \begin{cases} \rho(z^t) & \text{if } z^t \in \hat{\mathcal{Y}}_\epsilon^c \\ 0 & \text{otherwise} \end{cases}$. The expected value of $\rho(\tilde{Z}^t)$ is

$$\mathbb{E} \left[\rho \left(\tilde{Z}^t \right) \right] = \mathbb{E} \left[F \left(\tilde{Z}^{t+1} \right) \right] - \mathbb{E} \left[F \left(\tilde{Z}^t \right) \right].$$

Summing these expectations over time, we get

$$\sum_{k=0}^{t-1} \mathbb{E} \left[\rho \left(\tilde{Z}^k \right) \right] = \mathbb{E} \left[F \left(\tilde{Z}^t \right) \right] - F \left(z^0 \right).$$

Taking t to infinity and interchanging integration and summation we obtain

$$\mathbb{E} \left[\sum_{k=0}^{\infty} \rho \left(\tilde{Z}^k \right) \right] = \mathbb{E} \left[F \left(Z^\infty \right) \right] - F \left(z^0 \right).$$

From the definition of $\rho(\tilde{z}^k)$ we can write $\mathbb{E} \left[\sum_{k=0}^{\infty} \rho \left(\tilde{Z}^k \right) \right] \leq \mathbb{E} \left[K_\epsilon(-b_\epsilon) \right]$, thus obtaining the result

$$\mathbb{E} \left[K_\epsilon \right] \leq \frac{F(z^0) - \mathbb{E} \left[F \left(Z^\infty \right) \right]}{b_\epsilon} \leq \frac{F(z^0) - F^*}{b_\epsilon}$$

which is a finite number. This completes the proof. \square

References

- [1] A. M. Zoubir, V. Koivunen, Y. Chakhchoukh, M. Muma, Robust estimation in signal processing: A tutorial-style treatment of fundamental concepts, *IEEE Signal Processing Magazine* 29 (4) (2012) 61–80.
- [2] P. Oğuz-Ekim, J. Gomes, J. Xavier, P. Oliveira, Robust localization of nodes and time-recursive tracking in sensor networks using noisy range measurements, *Signal Processing, IEEE Transactions on* 59 (8) (2011) 3930–3942. doi:10.1109/TSP.2011.2153848.

- [3] P. Biswas, T.-C. Liang, K.-C. Toh, Y. Ye, T.-C. Wang, Semidefinite programming approaches for sensor network localization with noisy distance measurements, *Automation Science and Engineering*, *IEEE Transactions on* 3 (4) (2006) 360–371. doi:10.1109/TASE.2006.877401.
- [4] Y. Shang, W. Rumi, Y. Zhang, M. Fromherz, Localization from connectivity in sensor networks, *Parallel and Distributed Systems*, *IEEE Transactions on* 15 (11) (2004) 961–974. doi:10.1109/TPDS.2004.67.
- [5] C. Soares, J. Xavier, J. Gomes, Simple and fast convex relaxation method for cooperative localization in sensor networks using range measurements, *Signal Processing*, *IEEE Transactions on* 63 (17) (2015) pp. 4532–4543. doi:10.1109/TSP.2015.2454853.
- [6] Guo-Lin Sun, Wei Guo, Bootstrapping M-estimators for reducing errors due to non-line-of-sight (NLOS) propagation, *IEEE Communications Letters* 8 (8) (2004) 509–510.
- [7] J. Costa, N. Patwari, A. Hero III, Distributed weighted-multidimensional scaling for node localization in sensor networks, *ACM Transactions on Sensor Networks (TOSN)* 2 (1) (2006) 39–64.
- [8] T. Erseghe, A distributed and maximum-likelihood sensor network localization algorithm based upon a nonconvex problem formulation, *IEEE Transactions on Signal and Information Processing over Networks* 1 (4) (2015) 247–258. doi:10.1109/TSIPN.2015.2483321.
- [9] C. Soares, J. Xavier, J. Gomes, Distributed, simple and stable network localization, in: *Signal and Information Processing (GlobalSIP)*, 2014 IEEE Global Conference on, 2014, pp. 764–768. doi:10.1109/GlobalSIP.2014.7032222.
- [10] N. Piovesan, T. Erseghe, Cooperative localization in WSNs: a hybrid convex/non-convex solution, *IEEE Transactions on Signal and Information Processing over Networks* PP (99) (2016) 1–1. doi:10.1109/TSIPN.2016.2639442.
- [11] P. N. Alevizos, A. Bletsas, Network localization Cramér–Rao bounds for general measurement models, *IEEE Communications Letters* 20 (9) (2016) 1840–1843. doi:10.1109/LCOMM.2016.2585491.
- [12] C. E. O’Lone, H. S. Dhillon, R. M. Buehrer, A statistical characterization of localization performance in wireless networks, *IEEE Transactions on Wireless Communications* (2018). doi:10.1109/TWC.2018.2850310.
- [13] Y. Liu, Y. Shen, D. Guo, M. Z. Win, Network localization and synchronization using full-duplex radios, *IEEE Transactions on Signal Processing* 66 (3) (2018) 714–728. doi:10.1109/TSP.2017.2770090.

- [14] A. Shahmansoori, G. E. Garcia, G. Destino, G. Seco-Granados, H., Position and orientation estimation through millimeter-wave mimo in 5G systems, *IEEE Transactions on Wireless Communications* 17 (3) (2018) 1822–1835. doi:10.1109/TWC.2017.2785788.
- [15] A. Ihler, I. Fisher, J.W., R. Moses, A. Willsky, Nonparametric belief propagation for self-localization of sensor networks, *Selected Areas in Communications*, *IEEE Journal on* 23 (4) (2005) 809 – 819. doi:10.1109/JSAC.2005.843548.
- [16] J. Ash, R. Moses, Outlier compensation in sensor network self-localization via the EM algorithm, in: *Acoustics, Speech, and Signal Processing*, 2005. *Proceedings. (ICASSP '05)*. *IEEE International Conference on*, Vol. 4, 2005, pp. iv/749–iv/752 Vol. 4. doi:10.1109/ICASSP.2005.1416117.
- [17] F. Yin, A. Zoubir, C. Fritsche, F. Gustafsson, Robust cooperative sensor network localization via the EM criterion in LOS/NLOS environments, in: *Signal Processing Advances in Wireless Communications (SPAWC)*, 2013 *IEEE 14th Workshop on*, 2013, pp. 505–509. doi:10.1109/SPAWC.2013.6612101.
- [18] P. Forero, G. Giannakis, Sparsity-exploiting robust multidimensional scaling, *Signal Processing*, *IEEE Transactions on* 60 (8) (2012) 4118 –4134. doi:10.1109/TSP.2012.2197617.
- [19] S. Korkmaz, A.-J. van der Veen, Robust localization in sensor networks with iterative majorization techniques, in: *Acoustics, Speech and Signal Processing*, 2009. *ICASSP 2009*. *IEEE International Conference on*, 2009, pp. 2049 –2052. doi:10.1109/ICASSP.2009.4960017.
- [20] P. J. Huber, Robust estimation of a location parameter, *The Annals of Mathematical Statistics* 35 (1) (1964) 73–101.
- [21] S. Chen, J. Zhang, C. Xu, Robust distributed cooperative localization with nlos mitigation based on multiplicative convex model, *IEEE Access* 7 (2019) 112907–112920. doi:10.1109/ACCESS.2019.2915512.
- [22] S. Yousefi, X. W. Chang, B. Champagne, Distributed cooperative localization in wireless sensor networks without NLOS identification, in: *Positioning, Navigation and Communication (WPNC)*, 2014 *11th Workshop on*, 2014, pp. 1–6. doi:10.1109/WPNC.2014.6843290.
- [23] D. Blatt, A. Hero, Energy-based sensor network source localization via projection onto convex sets, *Signal Processing*, *IEEE Transactions on* 54 (9) (2006) 3614–3619. doi:10.1109/TSP.2006.879312.
- [24] M. R. Gholami, H. Wymeersch, E. G. Ström, M. Rydström, Wireless network positioning as a convex feasibility problem, *EURASIP Journal on Wireless Communications and Networking* 2011 (1) (2011) 161. doi:10.1186/1687-1499-2011-161.

- [25] C. Soares, J. Gomes, Robust dissimilarity measure for network localization, arXiv preprint arXiv:1410.2327 (2014).
- [26] A. Simonetto, G. Leus, Distributed maximum likelihood sensor network localization, *Signal Processing, IEEE Transactions on* 62 (6) (2014) 1424–1437. doi:10.1109/TSP.2014.2302746.
- [27] J.-B. Hiriart-Urruty, C. Lemaréchal, *Convex analysis and minimization algorithms*, Springer-Verlag Limited, 1993.
- [28] J. E. Falk, R. M. Soland, An algorithm for separable nonconvex programming problems, *Management science* 15 (9) (1969) 550–569.
- [29] M. Udell, S. Boyd, Bounding duality gap for problems with separable objective, *Computational Optimization and Applications* 64 (2) (2016) 355–378.
- [30] G. Destino, G. Abreu, On the maximum likelihood approach for source and network localization, *Signal Processing, IEEE Transactions on* 59 (10) (2011) 4954–4970. doi:10.1109/TSP.2011.2161302.
- [31] P. Oğuz-Ekim, J. P. Gomes, J. Xavier, M. Stošić, P. Oliveira, An angular approach for range-based approximate maximum likelihood source localization through convex relaxation, *IEEE Transactions on Wireless Communications* 13 (7) (2014) 3951–3964. doi:10.1109/TWC.2014.2314653.
- [32] A. Beck, M. Teboulle, A fast iterative shrinkage-thresholding algorithm for linear inverse problems, *SIAM journal on imaging sciences* 2 (1) (2009) 183–202.
- [33] R. Phelps, Convex sets and nearest points, *Proceedings of the American Mathematical Society* 8 (4) (1957) 790–797.
- [34] R. B. Bapat, *Graphs and matrices*, Springer, 2010.
- [35] F. R. Chung, *Spectral graph theory*, Vol. 92, American Mathematical Soc., 1997.
- [36] Y. Nesterov, A method of solving a convex programming problem with convergence rate $O(1/k^2)$, in: *Soviet Mathematics Doklady*, Vol. 27, 1983, pp. 372–376.
- [37] Y. Nesterov, *Introductory Lectures on Convex Optimization: A Basic Course*, Kluwer Academic Publishers, 2004.
- [38] D. Shah, *Gossip algorithms*, Now Publishers Inc, 2009.
- [39] A. Tarantola, *Inverse Problem Theory and Methods for Model Parameter Estimation*, Society for Industrial and Applied Mathematics, 2005. doi:10.1137/1.9780898717921.
URL <https://doi.org/10.1137/1.9780898717921>

- [40] P. Tsakalides, C. L. Nikias, Deviation from normality in statistical signal processing: Parameter estimation with alpha-stable distributions, A practical guide to heavy tails: statistical techniques and applications (1998) 379–404.
- [41] M. Grant, S. Boyd, CVX: Matlab software for disciplined convex programming, version 1.21, <http://cvxr.com/cvx> (Apr. 2011).
- [42] D. P. Bertsekas, J. N. Tsitsiklis, Parallel and distributed computation: Numerical methods, Prentice-Hall, Inc., Upper Saddle River, NJ, USA, 1989.
- [43] D. Jakovetic, J. Xavier, J. Moura, Cooperative convex optimization in networked systems: Augmented lagrangian algorithms with directed gossip communication, Signal Processing, IEEE Transactions on 59 (8) (2011) 3889–3902. doi:10.1109/TSP.2011.2146776.
- [44] W. Rudin, Principles of Mathematical Analysis, International series in pure and applied mathematics, McGraw-Hill, 1976.
- [45] D. Williams, Probability with martingales, Cambridge university press, 1991.